In vivo assembly of a genetically encoded artificial metalloenzyme for hydrogen production

Kassandra Naughton,† Regina E. Treviño, Peter J. Moore, Ashlee E. Wertz, J. Alex Dickson, and Hannah S. Shafaat*

Department of Chemistry and Biochemistry, The Ohio State University, Columbus, OH 43210, USA. *KEYWORDS Hydrogenases, nickel, electrochemistry, heterologous expression, metallation, E. coli.*

ABSTRACT: The genetic encoding of artificial enzymes represents a substantial advantage relative to traditional molecular catalyst optimization, as laboratory-based directed evolution coupled with high-throughput screening methods can provide

rapid development and functional characterization of enzyme libraries. However, these techniques have been of limited utility in the field of artificial metalloenzymes due to the need for *in vitro* cofactor metallation. Here, we report the development of methodology for *in vivo* production of nickel-substituted rubredoxin, an artificial metalloenzyme that is a structural, functional, and mechanistic mimic of the [NiFe] hydrogenases. Direct voltammetry on cell lysate establishes precedent for development of an electrochemical screen. This technique will be broadly applicable to the *in vivo* generation of artificial metalloenzymes that require a non-native metal cofactor, offering a route for rapid enzyme optimization and setting the stage for integration

of artificial metalloenzymes into biochemical pathways within diverse hosts.

The field of artificial metalloenzymes has experienced a dramatic surge over the last decade as molecular and microbiology tools have become more accessible and protein purification methods more straightforward.^{1,2} Enzyme optimization has benefited through application of directed evolution approaches, which take advantage of the short doubling times of hosts such as *E. coli*, providing access to enhanced reactivity.^{3,4} However, directed evolution relies on the proper assembly of the protein and cofactor within the heterologous organism. This latter requirement has stymied the application of directed evolution towards optimization of artificial metalloenzymes, which often use non-native metals or metallocofactors to carry out the desired chemistry. Because metal uptake and delivery is carefully controlled by all organisms, particularly for late transition metals,⁵ incorporation of non-native metals into overexpressed proteins has remained a challenge in the field. Recent advances have demonstrated in vivo incorporation of [4Fe-4S] clusters into de novo designed peptides and assembly of c-type hemes into engineered protein scaffolds. 6,7 These approaches harness the innate biochemical machinery present in *E. coli* for *c*-type cytochrome and iron-sulfur ([FeS]) cluster maturation. As an alternative method, insertion of a complete, fully synthetic cofactor has also been shown to result in proper in vivo assembly of [FeFe] hydrogenases, which has application to generating such enzymes from an array of organisms and within diverse hosts.⁸ However, the *in vivo* generation of a non-natural metallocofactor has yet to be reported.

In this work, we demonstrate the *in vivo* production of nickel-substituted rubredoxin (NiRd), an artificial metalloenzyme developed by our group for H_2 evolution. ^{9,10} The expressed and metallated enzyme is indistinguishable from chemically reconstituted NiRd, and an electrochemical screen has been developed for assessing hydrogenase activity from crude lysate. This work represents the first example of *in vivo* generation of an artificial metalloenzyme for energy conversion reactions and sets the stage for rapid evolution and optimization of diverse enzyme systems that utilize non-native metallocofactors, with potential for integration within biochemical pathways to tune downstream metabolic outputs.

Nickel-substituted rubredoxin is a structural, functional, and mechanistic mimic of the [NiFe] hydrogenases (**Figure 1A**).^{9,10} The highly active hydrogenase enzymes are found across the bacterial and archaeal kingdoms and feature a tetrathiolate nickel site bridged by two cysteine residues to a Fe(CO)(CN)₂ fragment (**Figure 1B**).^{11,12} The assembly of the native [NiFe] hydrogenases requires at least 6 accessory proteins, named HypA – HypF for the *E. coli* variants.¹³ The Fe fragment is synthesized by HypEF on the HypCD complex and must be inserted into the large catalytic sub-

unit prior to the nickel center. The high-affinity metallochaperones HypA and HypB are responsible for binding at least one Ni^{II} ion for transfer into the Fe-loaded subunit. The order of metal addition is critical for quantitative assembly of the functional cofactor.¹⁴ Cleavage of a Cterminal extended domain induces proper folding, and binding to the small, [FeS]-cluster containing subunit gives the fully assembled hydrogenase.^{15,16} The complexity of this pathway coupled with the still-unknown metabolic precursor of the CO ligand on Fe in the standard enzymes and, until recently, a lack of effective *in vivo* activity screens have hindered efforts to evolve hydrogenases in order to enhance specific activity traits.^{17,18}

On the other hand, the artificial enzyme scaffold, rubredoxin, is encoded on a pET21a(+) plasmid containing the lac promoter. The protein is expressed and retained in the cytosol, as confirmed through periplasmic lysis controls, and the 5.2 kDa protein is purified in the naturally occurring, iron-bound form through ion exchange chromatography. Acid precipitation of the fully purified protein is used to install non-native metals. While significantly simplified relative to the assembly, expression, and purifi-

cation of native [NiFe] hydrogenases, we hypothesized that we could obtain a crude assessment of NiRd activity and circumvent many of these steps by generating the nickelated protein within intact *E. coli* cells containing the Rd plasmid (**Figure 1C**).

Taking inspiration from prior work on nickel chaperones, which suggested that a [Ni(L-histidine)2] complex was the active substrate for nickel uptake through the NikABCDE transporter in E. coli, 20 NiCl₂ and L-histidine (L-His) were pre-mixed and added to terrific broth growth media once the cells reached log-phase at an OD_{600} of ~ 1 . The E. coli cells were grown in rich media and under aerobic conditions to retain high cell densities and rapid doubling times. Prior to addition of nickel, the cells were treated with EDTA, by analogy to literature protocols followed by others to control metallation.²¹ While nickel is typically considered toxic to cells,22 the addition of nickel up to a concentration of 20 mM only had a slight impact on cell optical density and resulted in a modest decrease in cell pellet size (Figure 1D). Serving as a visual indicator of metallation, the collected cells were noticeably green, reflecting the color of NiRd (Figure 1D, top inset). Controls

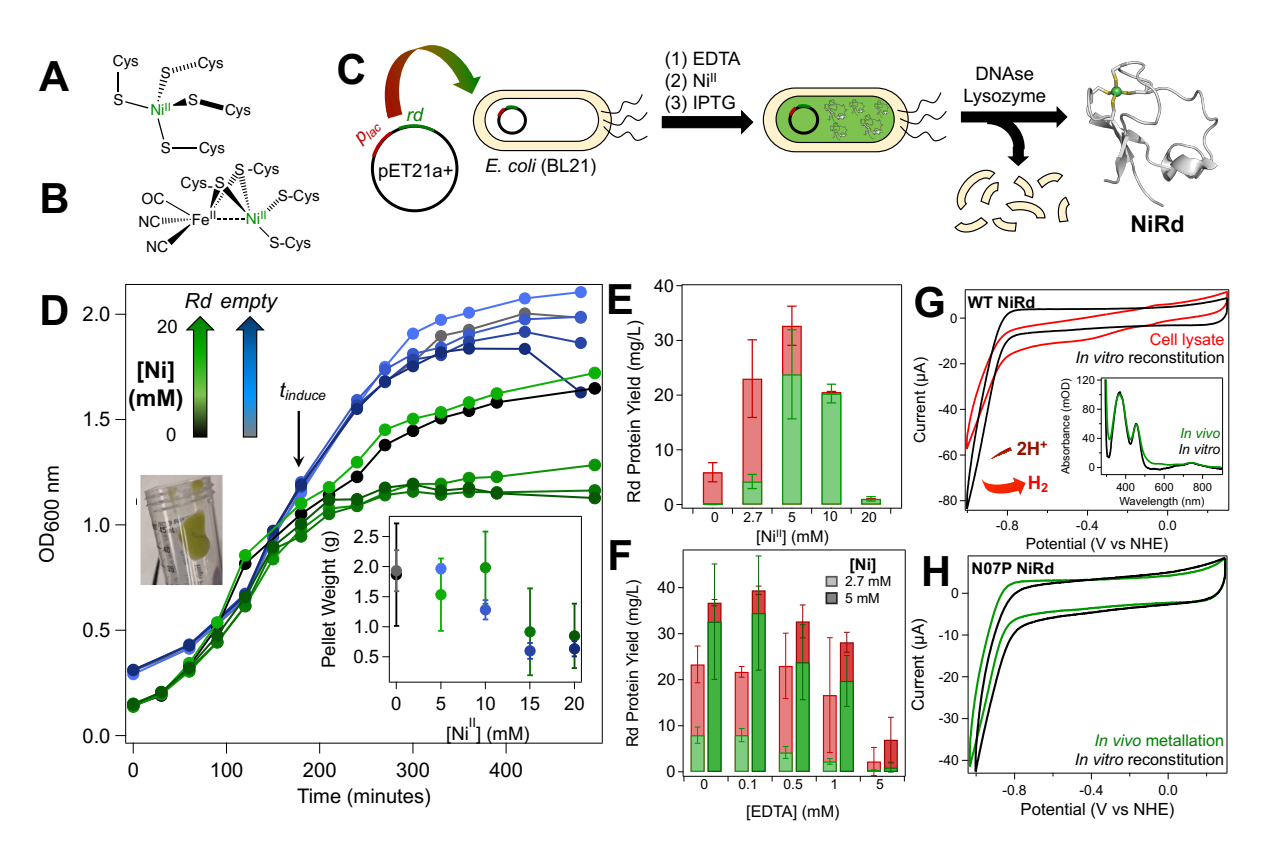


Figure 1. Active-site structures of (**A**) NiRd and (**B**) [NiFe] hydrogenase. (**C**) Putative nickel insertion pathway into heterologously expressed rubredoxin. (**D**) Growth curves of *E. coli* in the presence of added Ni (0, 5 mM, 10 mM, 15 mM, 20 mM; as indicated). At the time of induction (*black arrow*), 0.5 mM EDTA was added, followed by 500 μM L-His and Ni 30 min. later. Cells were transformed with either the Rd plasmid (*greens*) or an empty vector (*blues*). (**Top inset**) Photograph of harvested cells containing *in vivo* metallated NiRd. Green color is characteristic of the presence of NiRd. (*Bottom inset*) Average cell pellet weight as a function of added [Ni] (n ≥ 3 trials). Coloring as in (**D**). (**E**) − (**F**) Average rubredoxin yields (n ≥ 3 trials) as a function of added (**E**) [Ni^{II}] following addition of 0.5 mM EDTA and (**F**) [EDTA] preceding addition of 2.7 mM Ni^{II} (*light bars*) and 5 mM Ni^{II} (*dark bars*). Amounts of FeRd (*red*) and NiRd (*green*) measured using optical spectroscopy following initial purification. (**G**) Electrochemistry and (*inset*) optical spectra of WT NiRd generated through chemical reconstitution (*black*), purified following *in vivo* metallation (*green*), and crude cell lysate containing *in vivo* metallated NiRd (*red*). Arrow indicates catalytic current corresponding to H₂ evolution. (**H**) Electrochemistry on N07P NiRd generated through chemical reconstitution (*black*) and purified following *in vivo* metallation (*green*). Cyclic voltammogram of chemically reconstituted N07P NiRd was scaled to account for different electrode surface areas.

performed with an empty vector showed only a minor effect of Ni on growth curves or cell pellet mass, suggesting minimal toxicity of the added Ni^{II} salt towards bacterial growth. Cells lacking the Rd plasmid did not become green in the Ni-enriched growth media, consistent with metallated NiRd serving as the origin of the green color.

Lysis of the green NiRd-containing cells and one-step purification enabled quantification of the NiRd enzyme relative to the native, iron-bound protein (FeRd) as a function of added nickel and EDTA concentrations (Figure 1E-1F). Increasing amounts of NiRd and Rd levels overall were observed with up to 5 mM Ni^{II} in the growth media, with nearly complete selectivity for the nickel-bound protein observed with 10 mM added Ni^{II}; at 20 mM, lower protein yields were observed, likely as a result of the smaller pellet weights. The effects of added EDTA on the metallation distribution of Rd were also examined (Figure 1F). While the cellular growth curves and cell pellet sizes were unaffected by added EDTA (Figure S1), the metal distribution in Rd was significantly impacted. As addition of metal chelators such as EDTA or 1,10-phenanthroline prior to induction has previously been used by our lab and others to enhance production of apo-protein,21,23,24 presumably from scavenging labile cellular metals, it was hypothesized that the pre-induction incubation with EDTA facilitated enhanced nickel uptake and binding to Rd. Instead, EDTA appears to inhibit Ni binding to Rd, with decreasing yields of total metallated protein and NiRd relative to FeRd observed as the EDTA concentration is increased. This may be attributed to the higher binding affinity of EDTA for Ni over Fe, reflected in the relative ordering of the metals in the Irving-Williams series,25 which preferentially chelates Ni^{II} and renders it unavailable for incorporation into Rd. Upon optimization, nearly quantitative and selective metallation with nickel was observed for aerobic growth in rich media, suggesting little competition from intrinsic metals in the Terrific Broth. This approach resulted in high protein yields, bypassing many of the challenges associated with protein expression in minimal media or under anoxic conditions.26

The NiRd enzyme generated by in vivo metallation is indistinguishable from NiRd prepared through the standard metal substitution procedure, as evidenced by optical spectroscopy and protein electrochemistry (Figure 1G). Electrocatalysis by NiRd shows a distinct voltammetric signature, with currents in the cathodic region of the voltammogram exhibiting a linear response with increasing applied potential, characteristic of slow electron transfer relative to chemical processes, and parallel waves in the cathodic and anodic directions, indicating an absence of low-potential inactivation processes. 10,27 The currents directly correspond to the catalytic H2 evolution activity, while the position of the onset of the catalytic current indicates the overpotential for the reaction. In the purified wild-type (WT) NiRd, the onset potential for catalysis occurs at -800 mV vs. NHE at pH 4.0 (Figure 1G). Importantly, electrochemistry on crude cell lysate containing in vivo metallated NiRd showed the characteristic NiRd signals at low potentials, with an identical onset potential to that seen for purified protein. The large catalytic currents were clearly evident over the small non-catalytic background

signals of the endogenous redox cofactors in *E. coli*. Moreover, these experiments were performed on the benchtop rather than requiring a glovebox, indicating potential for extension to large-scale screening efforts. While electrochemical H+ reduction by NiRd has been shown to be insensitive to the presence of air,¹⁰ a nitrogen gas blanket was used over the electrochemical setup to minimize background O₂ reduction signals by the electrode.

In addition to metalation of WT NiRd, the application of the technique for *in vivo* metalation of more challenging mutants was explored. The N07P mutant possesses a more rigid metal-binding loop than WT Rd. As such, this mutant has been recalcitrant to metal substitution reactions, requiring many denaturation cycles to quantitatively replace iron with nickel. However, when the growth media for cells containing the N07P Rd plasmid was enriched in Ni^{II}, the cells became green after induction, indicating NiRd metalation. This was confirmed upon lysis and protein purification, which gave N07P in high yields and with identical electrochemical signals to those obtained from the reconstituted protein (**Figure 1H**).

The methods optimized in this work for the metallation of NiRd can be adapted to the study of a range of metalloenzymes. This project takes advantage of the high position of nickel on the Irving Williams series to promote strong, irreversible binding to Rd. Another strategy to prevent metallation by endogenous metals during expression has utilized competition with high concentrations of ions that are low on the Irving Williams series, such as MnII, to compete for Fe^{II} binding sites.^{28,29} Alternative approaches to promote binding of specific metals into given active sites may use metal selective chelators to facilitate uptake, as has been seen by the use of pyrithione to stimulate Cu uptake into E. coli.30 It is also important to consider the cell permeability of the selected chelator. By harnessing the ligation preferences of specific metals, it is anticipated that both natural and engineered metalloenzymes could be obtained through heterologous expression without the need for separate, in vitro reconstitution.

In addition to optimizing engineered systems, the facile in vivo metallation of Rd offers an example of how the study of model metalloenzymes can provide insight into the structure and function of native protein systems. In particular, the high affinity nickel chaperones in the [NiFe] hydrogenase assembly pathway are likely required to prevent the spontaneous binding of nickel into the empty tetrathiolate active site cavity, particularly during heterologous expression, which would occlude proper insertion of the Fe(CO)(CN)₂ fragment to give inactive enzyme.³¹ Moreover, the in vivo generation of NiRd in conjunction with facile electrochemical screening demonstrates the potential for generating artificial metalloenzymes within intact hosts, presenting the possibility to use directed evolution methods for practical, rapid optimization. Retention of the properly metallated enzyme within the cell rather than secretion into the media suggests that the protein can be further designed to interface with targeted metabolic pathways, merging synthetic and natural biology. For example, the gene for NiRd could be integrated within photosynthetic bacteria and coupled to light-driven electron transfer processes, offering a robust platform for production of solar hydrogen. The methodology presented in this work is anticipated to be broadly applicable for incorporation of metals ranging from Mn to Zn into the active sites of diverse artificial metalloenzyme scaffolds.

METHODS

Materials. All reagents used were manufactured by VWR International, Alfa Aesar, Bio Basic Canada Inc., Gold Biotechnology, or Sigma Aldrich unless specified otherwise. The Terrific Broth media was purchased as a premixed formulation from Research Products International. Protein purification columns were manufactured by Bio-Rad and GE Life Sciences.

Protein Expression and Purification. Expression and purification of chemically reconstituted rubredoxin as well as construction of the N07P mutant were performed as described previously. 9,10,27,32 All expression was carried out under aerobic growth conditions.

In vivo Incorporation of Nickel Expression and Purification. Expression of Rd was carried out in BL21 E. coli cells that had been transformed with a pET21a(+) vector containing the Rd gene downstream of the lac promoter. All media contained 70 mg/L carbenicillin to select for the transformed cells. A starter culture (5 mL) of E. coli in Terrific Broth (TB) was allowed to grow overnight at 37 °C prior to inoculation of 200 mL TB media. Cultures were allowed to grow at 25 °C until an OD_{600} of ~ 0.8 - 1 was reached. At this point, an EDTA solution was added to each of the sample flasks to a final concentration of 0.5 mM, unless otherwise noted. The flasks were allowed to shake at 25 °C and 200 RPM for 30 minutes, NiCl₂·6H₂O and Lhistidine were premixed to achieve the desired concentrations for a given experiment prior to addition to the culture. The flasks were then allowed to shake at 25 °C and 200 RPM for an additional 30 minutes. At this point, each culture was induced with IPTG at a final concentration of 1 mM, as described previously,10 and allowed to incubate overnight while shaking at 25 °C and 200 RPM.

Cells were harvested by centrifugation at 6800xg for 10 minutes at 4°C. The cells were washed by resuspension in a solution containing 50 mM Tris + 1 mM EDTA at pH 8.0 and collected by centrifugation. The supernatant was discarded, and the cell pellet was frozen at -80 °C for at least an hour. The pellets were lysed and purified by FPLC using ion-exchange chromatography with CHT and DEAE or HiTrap Q HP columns in series as described previously. The metalation state of Rd and purity were assessed using UV-Vis spectroscopy. 10 Added L-histidine was not found to affect the amount of NiRd produced up to 10 mM [L-His] (Figure S2).

Periplasmic Lysis. Periplasmic lysis controls to confirm cytosolic expression and metallation were performed as reported previously for periplasmic lysis methods optimized for other proteins.^{33,34} Following lysis, the supernatant containing periplasmically expressed proteins was assessed using optical spectroscopy. No signals indicative of NiRd were observed. After periplasmic lysis, the residual cellular material was treated with the normal lysis procedure. NiRd was obtained from this full cell lysis, as evidenced through optical characterization, and protein was

purified and tested in the same manner as described above.

Empty Vector Transformation and Cultivation. Chemically competent BL21 *E. coli* cells were transformed with an empty pET21a(+) vector following standard procedures. Cells were grown on solid agar media prior to cultivation in liquid culture. A single colony was selected for inoculation of a starter culture. Cells were grown in the presence of Ni^{II} and L-His as described above, with cell density monitored using OD₆₀₀ measurements and pellet size assessed following cell harvesting through centrifugation

Electrochemistry. Protein electrochemistry was performed as described previously.10 Briefly, purified protein was adsorbed on the surface of homemade pyrolytic graphite electrodes. Excess protein was pipetted off the surface of the electrode before immersion into a solution containing 50 mM acetate buffer, pH 4.0. Cyclic voltammograms were performed using a three-electrode set up with a Pt counter electrode and a mini Ag/AgCl reference electrode (Pine Instruments) and run in an anaerobic chamber (O₂ < 10 ppm, Vigor Technologies). Electrochemical experiments on cell lysate were performed under a blanket of nitrogen gas, ensuring all three electrodes were placed in close proximity, and included addition of nitrogen-sparged buffer containing 150 mM acetate, pH 4.0, to decrease the sample viscosity. Electrochemistry was run on cell lysate within 6-8 hrs of lysing the cells.

ASSOCIATED CONTENT

Supporting Information

Supplemental growth curves and histidine dependence. This material is available free of charge via the Internet at http://pubs.acs.org.

AUTHOR INFORMATION

Corresponding Author

*Hannah S. Shafaat, shafaat.1@osu.edu

Present Addresses

†Current address: University of Kentucky, Lexington, KY 40506, USA.

Author Contributions

All authors have given approval to the final version of the manuscript.

Funding Sources

NSF CHE-1454289

ACKNOWLEDGMENTS

We acknowledge the National Science Foundation (CHE-1454289) for supporting this research. RET would also like to acknowledge the Department of Education for a GAANN fellowship. We thank Dr. Jeffrey Slater for measuring the voltammograms of *in vitro* reconstituted NO7P NiRd.

ABBREVIATIONS

NiRd, nickel-substituted rubredoxin; FeS, iron-sulfur; wild-type, WT.

Conflicts of Interest

None.

REFERENCES

- (1) Schwizer, F.; Okamoto, Y.; Heinisch, T.; Gu, Y.; Pellizzoni, M. M.; Lebrun, V.; Reuter, R.; Köhler, V.; Lewis, J. C.; Ward, T. R. Artificial Metalloenzymes: Reaction Scope and Optimization Strategies. *Chem. Rev.* 2018, 118, 142–231 DOI: 10.1021/acs.chemrev.7b00014.
- (2) DiPrimio, D. J.; Holland, P. L. Repurposing metalloproteins as mimics of natural Metalloenzymes for small-molecule activation. *J. Inorg. Biochem.* 2021, 219, 111430 DOI: 10.1016/j.jinorgbio.2021.111430.
- (3) Arnold, F. H. Directed Evolution: Bringing New Chemistry to Life. Angewandte Chemie International Edition 2018, 57, 4143-4148 DOI: 10.1002/anie.201708408.
- (4) Zeymer, C.; Hilvert, D. Directed Evolution of Protein Catalysts. *Annual Review of Biochemistry* 2018, 87, 131–157 DOI: 10.1146/annurev-biochem-062917-012034.
- (5) Waldron, K. J.; Rutherford, J. C.; Ford, D.; Robinson, N. J. Metalloproteins and metal sensing. *Nature* 2009, 460, 823–830 DOI: 10.1038/nature08300.
- (6) Jagilinki, B. P.; Ilic, S.; Trncik, C.; Tyryshkin, A. M.; Pike, D. H.; Lubitz, W.; Bill, E.; Einsle, O.; Birrell, J. A.; Akabayov, B.; et al. In Vivo Biogenesis of a De Novo Designed Iron–Sulfur Protein. ACS Synth. Biol. 2020, 9, 3400–3407 DOI: 10.1021/acssynbio.0c00514.
- (7) Anderson, J. L. R.; Armstrong, C. T.; Kodali, G.; Lichtenstein, B. R.; Watkins, D. W.; Mancini, J. A.; Boyle, A. L.; Farid, T. A.; Crump, M. P.; Moser, C. C.; et al. Constructing a man-made c-type cytochrome maquette in vivo: electron transfer, oxygen transport and conversion to a photoactive light harvesting maquette. *Chem. Sci.* 2013, 5, 507–514 DOI: 10.1039/C3SC52019F.
- (8) Wegelius, A.; Land, H.; Berggren, G.; Lindblad, P. Semisynthetic [FeFe]-hydrogenase with stable expression and H2 production capacity in a photosynthetic microbe. *Cell Reports Physical Science* 2021, 100376 DOI: 10.1016/j.xcrp.2021.100376.
- (9) Slater, J. W.; Shafaat, H. S. Nickel-Substituted Rubredoxin as a Minimal Enzyme Model for Hydrogenase. J. Phys. Chem. Lett. 2015, 6, 3731–3736 DOI: 10.1021/acs.jpclett.5b01750.
- (10) Slater, J. W.; Marguet, S. C.; Monaco, H. A.; Shafaat, H. S. Going beyond Structure: Nickel-Substituted Rubredoxin as a Mechanistic Model for the [NiFe] Hydrogenases. J. Am. Chem. Soc. 2018, 140, 10250–10262 DOI: 10.1021/jacs.8b05194.
- (11) Lubitz, W.; Ogata, H.; Rüdiger, O.; Reijerse, E. Hydrogenases. *Chem. Rev.* **2014**, *114*, 4081-4148 DOI: 10.1021/cr4005814.
- (12) Shafaat, H. S. [NiFe] Hydrogenases: A Paradigm for Bioinorganic Hydrogen Conversion. In Reference Module in Chemistry, Molecular Sciences and Chemical Engineering; Elsevier, 2021.
- (13) Lacasse, M. J.; Zamble, D. B. [NiFe]-Hydrogenase Maturation. *Biochemistry* 2016, 55, 1689–1701 DOI: 10.1021/acs.biochem.5b01328.
- (14) Winter, G.; Buhrke, T.; Lenz, O.; Jones, A. K.; Forgber, M.; Friedrich, B. A model system for [NiFe] hydrogenase maturation studies: Purification of an active site-containing hydrogenase large subunit without small subunit. FEBS Lett. 2005, 579, 4292–4296 DOI: 10.1016/j.febslet.2005.06.064.
- (15) Hartmann, S.; Frielingsdorf, S.; Caserta, G.; Lenz, O. A membrane-bound [NiFe]-hydrogenase large subunit precursor

- whose C-terminal extension is not essential for cofactor incorporation but guarantees optimal maturation. *MicrobiologyOpen* **2020**, *9*, 1197–1206 DOI: 10.1002/mbo3.1029.
- (16) Sawers, R. G.; Pinske, C. NiFe-Hydrogenase Assembly. In Encyclopedia of Inorganic and Bioinorganic Chemistry; John Wiley & Sons, Ltd, 2017; pp 1–11.
- (17) Lacasse, M. J.; Sebastiampillai, S.; Côté, J.-P.; Hodkinson, N.; Brown, E. D.; Zamble, D. B. A whole-cell, high-throughput hydrogenase assay to identify factors that modulate [NiFe]-hydrogenase activity. J. Biol. Chem. 2019, 294, 15373–15385 DOI: 10.1074/jbc.RA119.008101.
- (18) Schulz, A.-C.; Frielingsdorf, S.; Pommerening, P.; Lauterbach, L.; Bistoni, G.; Neese, F.; Oestreich, M.; Lenz, O. Formyltetrahydrofolate Decarbonylase Synthesizes the Active Site CO Ligand of O2-Tolerant [NiFe] Hydrogenase. J. Am. Chem. Soc. 2020, 142, 1457–1464 DOI: 10.1021/jacs.9b11506.
- (19) Saint-Martin, P.; Lespinat, P. A.; Fauque, G.; Berlier, Y.; Le-Gall, J.; Moura, I.; Teixeira, M.; Xavier, A. V.; Moura, J. J. Hydrogen production and deuterium-proton exchange reactions catalyzed by Desulfovibrio nickel (II)-substituted rubredoxins. *Proc. Natl. Acad. Sci. U. S. A.* 1988, 85, 9378–9380.
- (20) Chivers, P. T.; Benanti, E. L.; Heil-Chapdelaine, V.; Iwig, J. S.; Rowe, J. L. Identification of Ni-(L-His)2 as a substrate for NikABCDE-dependent nickel uptake in Escherichia coli. *Metallomics* 2012, 4, 1043–1050 DOI: 10.1039/C2MT20139A.
- (21) Griese, J. J.; Roos, K.; Cox, N.; Shafaat, H. S.; Branca, R. M. M.; Lehtiö, J.; Gräslund, A.; Lubitz, W.; Siegbahn, P. E. M.; Högbom, M. Direct observation of structurally encoded metal discrimination and ether bond formation in a heterodinuclear metalloprotein. *Proc. Natl. Acad. Sci. U. S. A.* 2013, 110, 17189–17194 DOI: 10.1073/pnas.1304368110.
- (22) Macomber, L.; Hausinger, R. P. Mechanisms of nickel toxicity in microorganisms†. *Metallomics* 2011, 3, 1153–1162 DOI: 10.1039/c1mt00063b.
- (23) Miller, E. K.; Trivelas, N. E.; Maugeri, P. T.; Blaesi, E. J.; Shafaat, H. S. Time-Resolved Investigations of Heterobimetallic Cofactor Assembly in R2lox Reveal Distinct Mn/Fe Intermediates. *Biochemistry* 2017, 56, 3369–3379 DOI: 10.1021/acs.biochem.7b00403.
- (24) Parkin, S. E.; Chen, S.; Ley, B. A.; Mangravite, L.; Edmondson, D. E.; Huynh, B. H.; Bollinger, J. M. Electron Injection through a Specific Pathway Determines the Outcome of Oxygen Activation at the Diiron Cluster in the F208Y Mutant of Escherichia coli Ribonucleotide Reductase Protein R2. *Biochemistry* 1998, 37, 1124–1130 DOI: 10.1021/bi9723717.
- (25) Irving, H.; Williams, R. J. P. 637. The stability of transitionmetal complexes. *J. Chem. Soc.* 1953, No. 0, 3192–3210 DOI: 10.1039/JR9530003192.
- (26) Cai, M.; Huang, Y.; Yang, R.; Craigie, R.; Clore, G. M. A simple and robust protocol for high-yield expression of perdeuterated proteins in Escherichia coli grown in shaker flasks. *J Biomol NMR* 2016, 66, 85–91 DOI: 10.1007/s10858-016-0052-y.
- (27) Treviño, R. E.; Slater, J. W.; Shafaat, H. S. Robust Carbon-Based Electrodes for Hydrogen Evolution through Site-Selective Covalent Attachment of an Artificial Metalloen-zyme. ACS Appl. Energy Mater. 2020, 3, 11099–11112 DOI: 10.1021/acsaem.0c02069.
- (28) McBride, M. J.; Sil, D.; Ng, T. L.; Crooke, A. M.; Kenney, G. E.; Tysoe, C. R.; Zhang, B.; Balskus, E. P.; Boal, A. K.; Krebs, C.; et al. A Peroxodiiron(III/III) Intermediate Mediating Both N-Hydroxylation Steps in Biosynthesis of the N-Nitrosourea Pharmacophore of Streptozotocin by the Multi-domain Metalloenzyme SznF. J. Am. Chem. Soc. 2020, 142, 11818–11828 DOI: 10.1021/jacs.0c03431.

- (29) Kisgeropoulos, E. C.; Griese, J. J.; Smith, Z. R.; Branca, R. M. M.; Schneider, C. R.; Högbom, M.; Shafaat, H. S. Key Structural Motifs Balance Metal Binding and Oxidative Reactivity in a Heterobimetallic Mn/Fe Protein. *J. Am. Chem. Soc.* 2020, 142, 5338–5354 DOI: 10.1021/jacs.0c00333.
- (30) Zaengle-Barone, J. M.; Jackson, A. C.; Besse, D. M.; Becken, B.; Arshad, M.; Seed, P. C.; Franz, K. J. Copper Influences the Antibacterial Outcomes of a β-Lactamase-Activated Prochelator against Drug-Resistant Bacteria. ACS Infect. Dis. 2018, 4, 1019–1029 DOI: 10.1021/acsinfecdis.8b00037.
- (31) Hartmann, S.; Frielingsdorf, S.; Ciaccafava, A.; Lorent, C.; Fritsch, J.; Siebert, E.; Priebe, J.; Haumann, M.; Zebger, I.; Lenz, O. O2-Tolerant H2 Activation by an Isolated Large Subunit of a [NiFe] Hydrogenase. *Biochemistry* **2018**, *57*, 5339–5349 DOI: 10.1021/acs.biochem.8b00760.
- (32) Slater, J. W.; Marguet, S. C.; Gray, M. E.; Monaco, H. A.; Sotomayor, M.; Shafaat, H. S. Power of the Secondary Sphere:

- Modulating Hydrogenase Activity in Nickel-Substituted Rubredoxin. *ACS Catal.* **2019**, *9*, 8928–8942 DOI: 10.1021/acscatal.9b01720.
- (33) Manesis, A. C.; O'Connor, M. J.; Schneider, C. R.; Shafaat, H. S. Multielectron Chemistry within a Model Nickel Metalloprotein: Mechanistic Implications for Acetyl-CoA Synthase. J. Am. Chem. Soc. 2017, 139, 10328–10338 DOI: 10.1021/jacs.7b03892.
- (34) Manesis, A. C.; Musselman, B. W.; Keegan, B. C.; Shearer, J.; Lehnert, N.; Shafaat, H. S. A Biochemical Nickel(I) State Supports Nucleophilic Alkyl Addition: A Roadmap for Methyl Reactivity in Acetyl Coenzyme A Synthase. *Inorg. Chem.* 2019, 58, 8969–8982 DOI: 10.1021/acs.inorgchem.8b03546.

